Climate change increases carbon allocation to leaves in early leaf green-up

Fandong Meng[1#], Songbai Hong[2#], Jiawei Wang[2], Anping Chen[3,4], Yao Zhang[2], Yichen Zhang[2], Ivan A. Janssens[5], Jiafu Mao[6], Ranga B. Myneni[7], Josep Peñuelas[8,9], Shilong Piao[1,2]

[1] State Key Laboratory of Tibetan Plateau Earth System and Resources Environment (TPESRE), Institute of Tibetan Plateau Research, Chinese Academy of Sciences, 100085, Beijing China

[2] Sino-French Institute for Earth System Science, College of Urban and Environmental Sciences, Peking University, Beijing 100871, China

[3] Department of Biology, Colorado State University, Fort Collins, CO, USA

[4] Graduate Degree Program in Ecology, Colorado State University, Fort Collins, CO, USA.

[5] Department of Biology, University of Antwerp, Universiteitsplein 1, 2610 Wilrijk, Belgium

[6] Environmental Sciences Division and Climate Change Science Institute, Oak Ridge National Laboratory, Oak Ridge, TN 37831, USA

[7] Department of Earth and Environment, Boston University, Boston, MA 02215, USA

[8] CSIC, Global Ecology Unit CREAF-CSIC-UAB, Bellaterra, Barcelona 08193, Catalonia, Spain

[9] CREAF, Cerdanyola de Vallès, Barcelona 08193, Catalonia, Spain

# Contributed equally

Running Title: leaf carbon allocation under climate change

KEYWORDS

northern ecosystem, foliar carbon allocation, allocation ratio, optimal partitioning theory, terrestrial biosphere models

E-mail address

Fandong Meng[1#], fdmeng@pku.edu.cn; Songbai Hong[2#], songbaih@pku.edu.cn; Jiawei Wang[2], jiawei_wangvin@pku.edu.cn; Anping Chen[3,4], apchen1111@gmail.com; Yao Zhang[2], zhangyao@pku.edu.cn; Yichen Zhang[2], zhangyichen@stu.pku.edu.cn; Ivan A. Janssens[5], ivan.janssens@uantwerpen.be; Jiafu Mao[6], maoj@ornl.gov; Ranga B. Myneni[7], ranga.myneni@gmail.com; Josep Peñuelas[8,9], josep.penuelas@uab.cat, Josep.Penuelas@gmail.com; Shilong Piao[1,2], slpiao@pku.edu.cn

AUTHOR CONTRIBUTIONS

S. P designed the research; F. M and J. W performed analysis and created all figures; S. H, F. M and S. P created the first draft of the paper; and all authors contributed to the interpretation of the results and to the text.

DATA AVAILABILITY STATEMENT

Data and codes supporting the results are available in the Figshare: https://doi.org/10.6084/m9.figshare.21317637.

The type of article： Letters

The number of words in abstract: 143 words; **The number of words in main text:** 4649 words; **The number of references:** 52; **The number of figures:** 4

Correspondence

Shilong Piao, Sino-French Institute for Earth System Science, College of Urban and Environmental Sciences, Peking University, Beijing 100871, China. Tel: 010-62753298, Fax: 010-62753298, Email: slpiao@pku.edu.cn

Abstract

Global greening characterized by an increase in leaf area index (LAI) implies an increase in foliar carbon (C). Whether this increase in foliar C can be due to higher photosynthesis or higher allocation of C to leaves remains unknown under climate change. Here, we explored the divergent trends in foliar C accumulation and allocation during leaf green-up from 2000 to 2017 using satellite-derived LAI and solar-induced chlorophyll fluorescence (SIF). The accumulation of foliar C accelerated in early green-up period due to both increased photosynthesis and higher foliar C allocation driven by climate change. In the late stage, however, we detected negative decreased of foliar C accumulation and foliar C allocation. Such stage-variable trends in the accumulation and allocation of foliar C are not represented in current terrestrial biosphere models. Our results highlight that better representation of C allocation should be incorporated into models.

INTRODUCTION

Plant photosynthesis and respiration are two important fluxes affecting the terrestrial ecosystem carbon (C) cycle, and carbon allocation can affect these two processes by distribution assimilated C among plant parts (Lambers 1998; Chapin et al. 2002; Brüggemann et al. 2011). Many studies have investigated the assimilation of C and processes of respiration (Janssens et al. 2001; Keenan et al. 2013; Wehr et al. 2016; Bond-Lamberty et al. 2018), but much less effort has been devoted to the investigation of C allocation, i.e. the investment of photosynthetic products in different plant organs and functions (Brüggemann et al. 2011; Hartmann et al. 2020). Plants are often subjected to different resource limitations and stress factors and have different inherited life-history strategies, and hence the portfolios of C investment can change with shifts of dominant factors of resource limitations or stresses (Iwasa & Roughgarden 1984; Reich et al. 2014; Chen et al. 2020). For example, more C could be allocated to nonphotosynthetic parts such as stems for harvesting light or to roots for absorbing belowground resources, depending on the main type of resource limitation (Litton et al. 2007; Poorter et al. 2012; Guillemot et al. 2017).

The modifications of C allocation with environmental changes are important for both plant autoecological growth and ecosystem C cycles (Friedlingstein et al. 1999; Vicca et al. 2012; Konôpka et al. 2020). Most studies on plant C allocation, however, have been conducted at the autoecological level, with few at ecosystem or regional scales. Factors of global change, particularly the increase in CO_2 concentration, extreme droughts and increasing nitrogen (N) deposition, may profoundly alter stress factors and the broad-scale availability of plant resources (Finzi et al. 2007; Sardans et al. 2008; Kicklighter et al. 2019). Therefore, a better understanding of large-scale variations in the strategies of plant C allocation in response to

global change is essential for predicting vegetation dynamics and C cycles.

Recent advances in remote-sensing technology and data collection provide a potentially practical approach to investigate variations in the allocation of C between photosynthetic (leaves) and nonphotosynthetic (e.g. roots and stems) organs, both between years and within a growing season. In particular, seasonal plants grow leaves during the early part of growing season, but allocate more C to nonphotosynthetic organs at the peak of the season (Chapin 1991; Pantin et al. 2012; Tilman 2020). The exact allocation ratio between leaves and nonphotosynthetic organs during different stages of a growing season is difficult to obtain at broad scales, but remote sensing-based changes in the leaf area index (LAI) across these stages can be indicative of the amount of C allocated to leaves. Global greening identified using LAI has been widely observed under anthropogenic climate change (Zhu et al. 2016; Chen et al. 2019; Piao et al. 2020), but it remains unknown how different stages of a growing season contribute to this greening trend and how the allocation of C across different stages is regulated by climate change. Exploring these questions is important for increasing our understanding on the strategies used by plants to adapt to climate change and for improving the modeling of vegetation dynamics.

Here, we innovatively used the increases in LAI (ΔLAI) as a proxy for the allocation of C to leaves. We explored the interannual trends in ΔLAI in each month during the entire leaf green-up period in the Northern Hemisphere for 2000-2017, and further investigated how the trends were directly and indirectly regulated by environmental factors (e.g. temperature, soil-moisture content (SM) and solar radiation). Finally, we tested whether terrestrial biosphere models (TBMs) could identify the strategy used by plants to adapt to climate change by

adjusting C allocation at different stages of leaf green-up period. Our work found that the accumulation of foliar C accelerated in early green-up period and decreased in the late stage, but the TBMs did not capture the decreased trend due to inaccurate representation of C allocation strategy.

MATERIAL AND METHODS

Phenological metrics

We defined the period of leaf green-up period as the time between the start of the growing season (SOS) and the peak of the growing season (POS). SOS, defined as the date when the 2-band Enhanced Vegetation Index (EVI2) value first exceeded 15% (Gray et al. 2019), which is the phenological product of MCD12Q2 V6 calculated using data from the Moderate-resolution Imaging Spectroradiometer (MODIS) (downloaded from https://lpdaac.usgs.gov/products/mcd12q2v006/), available at 500-m spatial resolutions for 2001-2018. POS was defined as the date when annual LAI derived from the MOD15A2H v006 product was highest (details about the product are described below). The multi-year average dates of these two phenological metrics were converted from day of year into month of year, and then the duration of the ecosystem green-up period was calculated as the difference between POS and SOS.

Satellite-observed LAI

We used the LAI product of MOD15A2H v006 (https://lpdaac.usgs.gov/products/mod15a2hv006/) (Myneni et al. 2015). This product is

available at 500-m spatial and 8-d temporal resolutions for 2000-2017 (Yan et al. 2016). Monthly LAI was used to perform further analysis: on the one hand, it may reduce extreme values caused by clouds or aerosols (Verger et al. 2011) compared with multi daily LAI; on the other hand, it could compare with the modeled results with monthly temporal resolution. We first assigned each 8-d LAI data set to the month with the longest temporal overlap to obtain an accurate monthly LAI. For example, the LAI data set for 2 February was assigned to January due to only two out of eight days in February. We then extracted the monthly maximum as a proxy of monthly LAI, the monthly mean value was also used. Some types of vegetation lacking strong seasonal dynamics (e.g. evergreen forests and barren soils) were excluded based on the land-cover classification of MCD12C1 v006 (https://lpdaac.usgs.gov/products/mcd12c1v006/) (Friedl et al. 2010). We also excluded regions where annual maximum LAI occurred outside the March to October window. Another LAI product, CGLS (or the European Geoland2 Version 2 (GEOV2)); data input source: SPOT/VGT & PROBA-V (https://land.copernicus.eu/global/products/lai), was used to further verify the robustness of the results based on MODIS LAI. The spatial and temporal resolutions of LAI product of CGLS (or GEOV2) were 1-km and 10-d, respectively, available from 1999 to the present. We rescaled the two LAI products to a resolution of 0.5° to match the meteorological data sets.

Model-simulated LAI

The project "Trends and drivers of the regional scale sources and sinks of carbon dioxide" (TRENDY) V7 is a dynamic global vegetation model project that simulates a factorial set of the Dynamic Global Vegetation Model (DGVM) simulations

(http://dgvm.ceh.ac.uk/index.html), which was used to test how well state-of-the-art TBMs could reproduce satellite-observed changes in monthly foliar C accumulation and corresponding dominant drivers. We chose monthly composites of LAI of the third simulation (S3), including CO_2, climate and land use from 2000 to 2017. We used five models with spatial resolution of 0.5° (the same as that of the observed meteorological data sets and resampled LAI data): the Dynamic Land Ecosystem Model (DLEM), Lund-Postam-Jena General Ecosystem Simulator (LPJ-GUESS), Land surface Processes and eXchanges (LPX), Vegetation Integrative SImulator for Trace gases (VISIT) and the Vegetation Integrative Simulator for Trace gases (ISAM). The corresponding driving factors of these models are climatic forcing (the Climatic Research Unit (CRU) and the CRU Japanese 55-year Reanalysis (CRU-JRA55)), rising levels of atmospheric CO_2 from both ice core and atmospheric observations and land-use change (LUH2 data sets).

Meteorological data sets

The mean 2-m surface temperatures were acquired from CRU.TS4.04 at a spatial resolution of 0.5° and a monthly temporal resolution, which were interpolated from ground meteorological stations (https://crudata.uea.ac.uk/cru/data/hrg/cru_ts_4.04/cruts.2004151855.v4.04/) (Harris et al. 2020). The soil-moisture (SM) at a depth of 2-5 cm was acquired from the C3S dataset provided by European Centre for Medium-Range Weather Forecasts (ECMWF) v201812.0.0 at a spatial resolution of 0.25° and a monthly temporal resolution (https://cds.climate.copernicus.eu/cdsapp#!/dataset/satellite-soil-moisture?tab=overview).

Data for solar radiation were acquired from CRU-JRA v2.0, which is a combination of CRU

and a Japanese reanalyzed data set (JRA) (https://catalogue.ceda.ac.uk/uuid/7f785c0e80aa4df2b39d068ce7351bbb), at a spatial resolution of 0.5° and 6-hourly temporal resolution (Harris et al. 2014; Kobayashi et al. 2015). The SM data set was resampled to a spatial resolution of 0.5°.

Photosynthesis indicators

We used the synchronously simulated gross primary productivity (GPP) dataset from the five models described above to represent the photosynthetic activity. Solar-induced chlorophyll fluorescence (SIF), a probe of photosynthesis (Baker 2008), was used as a proxy for GPP in the satellite-observed data analysis due to the lack of long-term observational GPP data at large scale. The data set for contiguous SIF (CSIF) dataset was trained by a neural networks method using SIF from Orbiting Carbon Observatory-2 (OCO-2) and MCD43C1 v6 reflectance as input variables (Zhang et al. 2018), which has a 4-d temporal and a 0.05^{o} spatial resolutions, available from 2000 to 2020 (https://doi.org/10.17605/OSF.IO/8XQY6). Therefore, it makes up for the coarse spatiotemporal resolution and high uncertainty in the current SIF data set (Zhang et al. 2018).

Data analysis

We used the increase in LAI (ΔLAI) in each month and throughout green-up period to indicate the net allocation of C to leaves because the respired C was not considered here (hereafter leaf C). ΔLAI during green-up period was defined as annual maximum LAI minus LAI in the month before SOS, and monthly ΔLAI was calculated as (Fig. S1a):

$$\Delta LAI = LAI_t - LAI_{t-1} \quad \text{Eq. 1}$$

Because foliar growth is irreversible during the green-up period (Pantin et al. 2012) and there were few pixels with ΔLAIs <0 (only 0.07~2.4%, Fig. S2), So these pixels were discarded from our analysis.

Linear regression was used to identify the interannual trends in ΔLAI throughout the entire study period (Fig. S1b, Eqn2):

$$(\Delta LAI)_i = a_i * (Time) + b_i \quad \text{Eq. 2}$$

where time is the number of years from 2000 to 2017 for pixel i, a_i is the temporal trend in ΔLAI for pixel i, b_i is the intercept for pixel i. For the pixels with positive trends in green-up period ΔLAI, we further defined the month contributing the most to the increase in ΔLAI (the month with largest positive trends in monthly ΔLAI) during the green-up period as the dominant month (TDM). The time between SOS and TDM is shown in Fig. 1g. We further examined the temporal autocorrelation of ΔLAI, we found that there was no evident temporal autocorrelation of ΔLAI for different months (Fig. S3).

The amount of C allocated to leaves (C_{leaf}) depends on the total amount of assimilated photosynthetic C assimilation (C_{total}) and the proportion of C_{total} that is allocated to leaves (P_{leaf}):

$$C_{leaf} = C_{total} \times P_{leaf} \quad \text{Eq. 3}$$

To disentangle the relative importance of these two drivers. We built two different statistical models by the partial correlation analysis. The partial correlation analysis is a method that can access the net correlation coefficient between two variables by setting other synergistic variables as the controlling variables. The first model is driven by climate factors including temperature, SM and solar radiation. It consisted of the integrated effects of both C_{total} and P_{leaf}

on C_{leaf}. Note that the lagged effects of the climate factors were also considered by means of the preseason period. The preseason, defined as the period which most strongly affects phenological events (Menzel et al. 2006), was determined as the period preceding an event that exhibited the largest absolute value of partial correlation coefficient between ΔLAI and a climate factor, after controlling for the other climatic factors.

The second model is driven by including photosynthesis as the mediator between climate factors and C_{leaf}. The indicator of photosynthesis is substituted as SIF for observational data and modeled GPP for modeled data. The photosynthesis in the partial correlation analysis indicated the effect of C_{total} on C_{leaf}, and the remaining effects represented the effect of P_{leaf} which is affected by climate factors on C_{leaf} based on the Eq. 3. The difference between the partial correlation analyses with and without the indicator of photosynthesis then represented the climate effect on C_{leaf} by affecting C_{total}. The same analysis was conducted for the modeled data. The effect of atmospheric VPD (CRU) (Harris et al. 2020) was also examined in the partial correlation analysis.

RESULTS

Changes in leaf C accumulation during the green-up period and their climate drivers

The green-up period ΔLAI (annual maximum LAI minus LAI in the month before the start of the growing season (SOS)) showed positive trends in most areas (71% of pixels) from 2000 to 2017 (Fig. 1a). Monthly ΔLAI (LAI in the current month minus LAI in the previous month), which is indicative of the inter-month rate of foliar C accumulation, however, had divergent trends across different months (Fig. 1b-e). For example, the trends in ΔLAI in Europe were

widely positive in April (Fig. 1b) but negative in May (Fig. 1c). ΔLAI had widespread uptrends in North America in May (Fig. 1c) and June (Fig. 1d), but widespread uptrends in Siberia only in June (Fig. 1d). This spatiotemporal heterogeneity of ΔLAI trends is associated with vegetation phenology: earlier phenology coincided with the earlier occurrence of positive ΔLAI trends, and vice versa. Indeed, if we defined the month contributing the most to the uptrend in ΔLAI in green-up period as the dominant month (TDM) (Fig. 1f), the duration from SOS to TDM was no more than one month in most areas (Fig. 1g). Surprisingly, 78% of all pixels in July showed negative trends in ΔLAI during 2000-2017 (Fig. 1e), despite the widespread increase in July LAI over the same period (Fig. S4d). We also tested the robustness of the above results obtained with the Moderate-resolution Imaging Spectroradiometer (MODIS) LAI product (MOD15A2H v006) using the monthly mean value as a proxy of monthly LAI (Fig. S5) and the Copernicus Global Land Service (CGLS) LAI product (data input source: the 'Satellite Pour l'Observation de la Terre' (SPOT) VEGETATION (SPOT/VGT) & the Project for On-Board Autonomy–Vegetation (PROBA-V)), which consistently indicated that foliar C accumulation generally had positive trends in the early stage of green-up but negative trends in late stages (Fig. S6).

We further performed partial correlation analyses between ΔLAI and climatic factors (temperature, SM and radiation) to understand how changes in climatic variables may contribute to the observed trends in foliar C accumulation during each month of the green-up period (Fig. 2a-h). Since the climate of the preceding months (preseason) can also influence phenological dates and affect the rate of foliar C accumulation, we also included potential lagged effects of the climatic variables on ΔLAI in the analyses (Fig. S7). The results suggested

256 that temperature was the dominant climatic driver for ΔLAI in the early green-up stage (Fig. 2).
257 For example, temperature in regions with the earliest onset of spring phenology (such as Europe
258 and central and eastern North America, Fig. S8) was often the dominant climatic factor
259 positively associated with ΔLAI in April, the month of spring onset, after controlling for SM
260 and solar radiation (Figs. 2a, S9a). This dominant and positive effect of temperature on ΔLAI
261 extended to higher latitudes in May, including Canada and Siberia (Figs. 2b, S9b), but was not
262 observed in the northernmost regions until June (Figs. 2c, S9c). SM played a key role in
263 regulating ΔLAI in May for regions with continental climate such as inland Eurasia and North
264 America (Figs. 2b, S9f), especially where the dominant type of vegetation is temperate and
265 semi-arid grassland (Fig. S10). For these regions, both SM and temperature jointly regulated
266 foliar C accumulation in June, but with opposite effects on ΔLAI (Figs. 2, S9). Across the whole
267 study area, SM positively affected ΔLAI in 56% of the pixels (Fig. S9g), and temperature was
268 generally negatively correlated with ΔLAI (Fig. S9c). These contrasting effects of SM and
269 temperature on ΔLAI were even more widespread in July, when ΔLAI and SM were positively
270 correlated in 65% of the pixels (Fig. S9h) and ΔLAI and temperature were negatively correlated
271 in 66% of the pixels (Fig. S9d).
272
273 **Climate effects on leaf C assimilation and allocation**
274 Interestingly, SIF was more strongly correlated with ΔLAI than the climatic variables in the
275 early green-up stage (Fig. 2). Temperature had a weakened, but still positive, effect on ΔLAI
276 after controlling for SIF (Figs. S11-13). In the late stage of the green-up period (May at low
277 latitudes and June and July at higher latitudes), the correlation between ΔLAI and SIF was

generally weaker and even nonsignificant in most areas (Figs. 2, S11). The correlation between ΔLAI and temperature in this late green-up stage did not change when SIF was or was not controlled for (Figs. S11-13).

Assessing the performance of TBMs in C allocation simulations

The partial correlation analysis between ΔLAI and climatic factors (temperature, SM and radiation) with a potential lagged effect (Fig. S14) indicated that the models could generally reproduce the apparent response of foliar C accumulation to climate change (Figs. 3e-l, S15). Nonetheless, the partial correlations between modeled ΔLAI and temperature in the late green-up stage were more negative than the satellite-based results (comparing Figs. S15 and S9), suggesting a potentially overestimated apparent sensitivity of ΔLAI to temperature by the models. These models also underestimated the apparent influence of SM on foliar C accumulation (Fig. S15), especially in temperate and semi-arid grasslands, where satellite data indicated strong correlations between ΔLAI and SM (Fig. S9).

We also assessed whether the models could reproduce the climatic regulation of C_{total} and P_{leaf} by including modeled gross primary productivity (GPP) as an independent variable in the partial correlation analyses (Figs. 3m-t, S16). The results suggested that the models generally replicated the weak effects of solar radiation on foliar C accumulation by P_{leaf} (Fig. S17) but did not adequately simulate the changes in strategy of foliar allocation (i.e. P_{leaf}) due to variations in temperature and SM (Figs. 3m-t, S16).

DISCUSSIONS

Our study provides the first understanding on vegetation foliar C accumulation and allocation in large scale. We found that foliar C accumulation is increasing during the early stage of green-up but decreasing in the late green-up stage on the northern ecosystem over the past 18 years from 2000 to 2017. Climate change can affect foliar C accumulation (C_{leaf}) by impacting on C_{total} (Wehr et al. 2016; Gampe et al. 2021) and/or P_{leaf} (Iwasa & Roughgarden, 1984; Reich et al., 2014; Chen et al., 2020) (Fig. 4). In early stage, we found that an increase in photosynthesis over the past 18 years was the primary factor contributing to the increase in foliar C accumulation, but temperature could still contribute to the increase in C_{leaf} even after accounting for its direct impact on C_{total}, likely by affecting P_{leaf}. This preference of plants to allocate more C to leaves in the early green-up stage under warming is likely because vegetation productivity is more limited by the foliar surface than by the access of roots to soil water and nutrients (Chapin et al. 2002; Chen et al. 2020).

In the late stage, the increase in foliar photosynthesis did not necessarily increase the accumulation of foliar C. As the canopies close in this stage, vegetation productivity is more constrained by the availability of water and nutrients than by the number of leaves for photosynthesis, resulting in more C invested in nonphotosynthetic plant organs for acquiring resources (Chapin et al. 2002; Chen et al. 2020). An increase in temperature during this late green-up stage generally increases plant autotrophic respiration (Chapin et al. 2002) more than it does to the increase in photosynthesis because of the reduced optimal temperature of photosynthesis by stomatal closure (Drake et al. 2016). Continuing the allocation of more C to leaves under temperature increases in this late green-up stage is therefore not economical (Bloom et al. 1985; McCarthy & Enquist 2007). Warming can also increase atmospheric vapor-

pressure deficits (VPDs) and induce water stress (Yuan et al. 2019), which can become increasingly important in limiting vegetation productivity from the early to late green-up stages and thus diverting more C investment to organs for acquiring and transporting water (Guillemot et al. 2017; Hartmann et al. 2020). This indirect effect of temperature by increasing VPD was particularly possible in Europe (Fig. S18b) and North America (Fig. S18d), where the significantly negative correlation between ΔLAI and temperature was weakened and even disappeared when VPD was further controlled for.

Regarding the impacts of SM and solar radiation on foliar C accumulation during green-up period, solar radiation noticeably affected C_{leaf} in May (Fig. S9) by increasing photosynthetic C_{total} (Figs. S9, S11). In contrast, SM could potentially affect C_{leaf} by affecting both C_{total} and P_{leaf} (Figs. S9, S11), which is worth further studies. Increasing the availability of soil water can increase C_{total} (Reich et al. 2018; Liu et al. 2020), but little is known about how variations in SM may also lead to trade-offs in C allocation between leaves and other organs (Bloom et al. 1985; Tilman 2020). Several mechanisms may have contributed to the observed impact of SM on P_{leaf} (Fig. 4). First, high SM can relieve plant water stress and reduce the need for C investment for acquiring and transporting water (Litton et al. 2007; Poorter et al. 2012; Guillemot et al. 2017), which can shift more C to leaves and hence increase P_{leaf}. Second, an increase in SM can increase the activities of soil microbes and accelerate the mineralization of soil N and phosphorus (Keuper et al. 2012; Finger et al. 2016), which can also reduce the need of allocating more C to root systems (Litton et al. 2007; Poorter et al. 2012; Guillemot et al. 2017). Meanwhile, increasing N availability could stimulate plants to allocate more C to leaves for assimilating more C to maintain the C: N stoichiometric ratio. Third, when SM is low, a

decrease in P_{leaf} saves water and reduces respiratory C loss (Metcalfe et al. 2010). Fourth, root exudation can also compete with leaves for C under drought, because thirsty tree roots exude more C (Heinemeyer et al. 2012; Preece et al. 2018).

Correct schemes for C allocation simulations are essential for the accurate prediction of vegetation dynamics and ecosystem C cycles by process-based TBMs. However, TBMs could well capture the early stage of foliar C allocation but overestimate it in the late stage of green-up. Parallel analysis like observations, the overestimation of foliar C allocation during the late stage of green-up was caused by the neglect of the SM effect on foliar C accumulation. The actual process was that the models generally replicated the weak effects of solar radiation on foliar C accumulation by P_{leaf} (Fig. S17) but did not adequately simulate the changes in strategy of foliar allocation (i.e. P_{leaf}) due to variations in temperature and SM (Figs. 3m-t, S16), which were likely the cause of the biases in the modeled apparent sensitivities of foliar C accumulation to these climatic variables, for three reasons.

First, the models overestimated the link between photosynthesis and C allocation to leaves in the late stage of green-up (Figs. 3, S16), which may explain why the models could not reproduce the widespread downward trends in ΔLAI during July (Fig. 3d, 38% pixels for the models versus 78% pixels for the satellite-based results exhibiting negative trends in ΔLAI, Fig. 1e). The satellite-based findings indicated that the increase in foliar photosynthesis did not necessarily increase foliar C accumulation in the late stage of green-up. Four of the five models (all except LPX, Fig. S19), however, generated strong positive correlations between GPP and ΔLAI in this stage, which could lead to false positive feedbacks that in turn lead to the overestimation of vegetation productivity. Second, three of the models (LPJ-GUESS, LPX and

366 VISIT, Fig. S20) replicated the negative effect of temperature on foliar C accumulation by
367 influencing P_{leaf} in the late stage of green-up but overestimated the strength of this negative
368 effect. The other two models either produced a positive effect of temperature on P_{leaf} (and
369 consequently on foliar C accumulation) in the late stage of green-up or a weak correlation
370 between ΔLAI and temperature throughout green-up period, both in contrast to the satellite-
371 derived results. These models may have skewed the trade-offs of C allocation between organs
372 under changing temperature. Third, surprisingly, none of the five models reproduced the
373 positive effect of SM on P_{leaf} and ΔLAI (Fig. S21), which may be another reason for the
374 mismatch between the models and satellite observations in the ΔLAI trend in the late stage of
375 green-up period. Optimizing the response of C allocation in TBMs to different drought stresses
376 would likely improve their performance.

377 There are also uncertainties related to representation of leaf C and LAI product. The proxy
378 of leaf C by LAI may cause an uncertainty in evaluating its variation, for specific leaf area (the
379 ratio of fresh leaf area to dry leaf biomass) is not constant. SLA changes with environments,
380 then may lead to a non-linear relationship of LAI-leaf C. However, no long-term dataset of SLA
381 in current observations or databases (such as TRY database) allows us to explore its variation
382 over time. An experimental study showed a slight response of SLA over time due to the opposite
383 effect of temperature and CO2 (Tjoelker et al., 1999). Future progresses in observing networks
384 of plant traits may contribute to solving this uncertainty. In addition, our analyses were
385 conducted at a spatial resolution of 0.5° × 0.5°, which is fairly coarse and may lead to some
386 uncertainties. First, it is difficult for us to distinguish whether the changes in LAI are attributed
387 climate change or vegetation type shift for a mixed pixel, especially in the ecological transition

zones. Second, the driving mechanisms at local-scale can be masked by broad-scale patterns based on ecological scaling theory (Levin et al., 1992; Bradford et al., 2017). Accordingly, our findings call to test the mechanisms controlling leaf C allocation with full scope from population to community and from regional to global scales in future studies.

In summary, we provide the first account of how foliar C accumulation and allocation may have changed during different stages of the green-up period from 2000 to 2017 at the landscape level using data sets of satellite-derived LAI and SIF. Our results highlighted an accelerating accumulation of foliar C during the early stage of green-up due to the increases in both total photosynthesis and the proportion of photosynthetic C allocated to leaves under recent climate change. In contrast, foliar C accumulation during the late green-up stage showed a decreasing trend. The divergent trends of foliar C accumulation in the early versus late stages of green-up are consistent with the optimal partitioning theory, which has been verified at the level of individual plants, but never at the broader landscape level before. This landscape-level optimized C allocation scheme between photosynthetic and nonphotosynthetic plant organs in response to climate changes has important implications for the global change modeling community. TBMs are currently inadequate for modeling the response of C allocations to climatic variations at different stages of vegetation growth, in particular the overestimation of foliar C allocation during the late stage of green-up and the neglect of the SM effect on foliar C accumulation. This lack of capacity in C allocation simulations may be one of the sources for the large uncertainties in modeling C cycle responses to climate change.

Reducing model uncertainties requires better parameterization and description of the C allocation scheme and its dynamics with vegetation seasonal cycles and climate change. Clearly,

integrated studies combining data from manipulative field experiments and long-term observations of plant C allocation are valuable for model development and verifications. On the other hand, however, ecological theories of optimal resource acquisition provide critical guidelines in developing and refining climate change adapted allocation schemes used in TBMs, which can also be extended to other components (such as roots) where empirical experimental and observational data are even more difficult to obtain over broader scales. Furthermore, while direct evidence from in-situ long-term biomass observations is lacking, our findings will inspire new research, especially that using networks of coordinated ground monitoring (e.g. the NEON system), to further test the hypothesis and improve our understanding of carbon allocation under climate change.

CONFLICT OF INTEREST

There are no conflicts of interest to declare.

ACKNOWLEDGEMENTS

This study was supported by the National Natural Science Foundation of China (41988101), the Second Tibetan Plateau Scientific Expedition and Research (STEP) program (grant no. 2019QZKK0405). A.C. was supported by an Oak Ridge National Lab subcontract (4000167205)

REFERENCES

Baker, N.R. (2008) Chlorophyll fluorescence: a probe of photosynthesis in vivo. *Annual Review of Plant Biology*, 59, 89-113.

Bloom, A.J., Chapin III, F.S. & Mooney, H.A. (1985) Resource limitation in plants-an economic analogy. *Annual Review of Ecology and Systematics*, 16, 363-392.

Bond-Lamberty, B., Bailey, V.L., Chen, M., Gough, C.M. & Vargas, R. (2018) Globally rising soil heterotrophic respiration over recent decades. *Nature*, 560, 80-83.

Bradford, M. A., G. Veen, A. Bonis, E. M. Bradford, A. T. Classen, J. H. C. Cornelissen, et al. (2017) A test of the hierarchical model of litter decomposition. *Nature Ecology & Evolution*, 1: 1836-1845.

Brüggemann, N., Gessler, A., Kayler, Z., Keel, S., Badeck, F., Barthel, M. et al. (2011) Carbon allocation and carbon isotope fluxes in the plant-soil-atmosphere continuum: a review. *Biogeosciences*, 8, 3457-3489.

Chapin, F.S. (1991) Integrated responses of plants to stress. *Bioscience*, 41, 29-36.

Chapin, F.S., Matson, P.A., Mooney, H.A. & Vitousek, P.M. (2002) Principles of terrestrial ecosystem ecology. 132-134.

Chen, C., Park, T., Wang, X., Piao, S., Xu, B., Chaturvedi, R.K. et al. (2019) China and India lead in greening of the world through land-use management. *Nature Sustainability*, 2, 122-129.

Chen, R., Ran, J., Hu, W., Dong, L., Ji, M., Jia, X. et al. (2020) Effects of biotic and abiotic factors on forest biomass fractions. *National Science Review*, 0, nwab02.

Drake, J.E., Tjoelker, M.G., Aspinwall, M.J., Reich, P.B., Barton, C.V., Medlyn, B.E. et al.

(2016) Does physiological acclimation to climate warming stabilize the ratio of canopy respiration to photosynthesis? *New Phytologist*, 211, 850-863.

Finger, R.A., Turetsky, M.R., Kielland, K., Ruess, R.W., Mack, M.C. & Euskirchen, E.S. (2016) Effects of permafrost thaw on nitrogen availability and plant–soil interactions in a boreal Alaskan lowland. *Journal of Ecology*, 104, 1542-1554.

Finzi, A.C., Norby, R.J., Calfapietra, C., Gallet-Budynek, A., Gielen, B., Holmes, W.E. et al. (2007) Increases in nitrogen uptake rather than nitrogen-use efficiency support higher rates of temperate forest productivity under elevated CO2. *Proceedings of the National Academy of Sciences*, 104, 14014-14019.

Friedl, M.A., Sulla-Menashe, D., Tan, B., Schneider, A., Ramankutty, N., Sibley, A. et al. (2010) MODIS Collection 5 global land cover: Algorithm refinements and characterization of new datasets. *Remote Sensing of Environment*, 114, 168-182.

Friedlingstein, P., Joel, G., Field, C.B. & Fung, I.Y. (1999) Toward an allocation scheme for global terrestrial carbon models. *Global Change Biology*, 5, 755-770.

Gampe, D., Zscheischler, J., Reichstein, M., O'Sullivan, M., Smith, W.K., Sitch, S. et al. (2021) Increasing impact of warm droughts on northern ecosystem productivity over recent decades. *Nature Climate Change*, 11, 772-779.

Gray, J., Sulla-Menashe, D. & Friedl, M.A. (2019) User guide to collection 6 modis land cover dynamics (mcd12q2) product. *NASA EOSDIS Land Processes DAAC: Missoula, MT, USA*, https://lpdaac.usgs.gov/products/mcd12q2v006/.

Guillemot, J., Francois, C., Hmimina, G., Dufrêne, E., Martin-StPaul, N.K., Soudani, K. et al. (2017) Environmental control of carbon allocation matters for modelling forest growth.

New Phytologist, 214, 180-193.

Harris, I., Jones, P.D., Osborn, T.J. & Lister, D.H. (2014) Updated high-resolution grids of monthly climatic observations−the CRU TS3. 10 Dataset. *International Journal of Climatology*, 34, 623-642.

Harris, I., Osborn, T.J., Jones, P. & Lister, D. (2020) Version 4 of the CRU TS monthly high-resolution gridded multivariate climate dataset. *Scientific Data*, 7, 109.

Hartmann, H., Bahn, M., Carbone, M. & Richardson, A.D. (2020) Plant carbon allocation in a changing world–challenges and progress: introduction to a virtual issue on carbon allocation. *New Phytologist*, 227, 981-988.

Heinemeyer, A., Wilkinson, M., Vargas, R., Subke, J.-A., Casella, E., Morison, J.I. et al. (2012) Exploring the" overflow tap" theory: linking forest soil CO 2 fluxes and individual mycorrhizosphere components to photosynthesis. *Biogeosciences*, 9, 79-95.

Iwasa, Y. & Roughgarden, J. (1984) Shoot/root balance of plants: optimal growth of a system with many vegetative organs. *Theoretical population biology*, 25, 78-105.

Janssens, I., Lankreijer, H., Matteucci, G., Kowalski, A., Buchmann, N., Epron, D. et al. (2001) Productivity overshadows temperature in determining soil and ecosystem respiration across European forests. *Global Change Biology*, 7, 269-278.

Keenan, T.F., Hollinger, D.Y., Bohrer, G., Dragoni, D., Munger, J.W., Schmid, H.P. et al. (2013) Increase in forest water-use efficiency as atmospheric carbon dioxide concentrations rise. *Nature*, 499, 324-327.

Keuper, F., van Bodegom, P.M., Dorrepaal, E., Weedon, J.T., van Hal, J., van Logtestijn, R.S. et al. (2012) A frozen feast: Thawing permafrost increases plant-available nitrogen in

494 subarctic peatlands. *Global Change Biology*, 18, 1998-2007.
495 Kicklighter, D.W., Melillo, J.M., Monier, E., Sokolov, A.P. & Zhuang, Q. (2019) Future
496 nitrogen availability and its effect on carbon sequestration in Northern Eurasia. *Nature*
497 *Communications*, 10, 1-19.
498 Kobayashi, S., Ota, Y., Harada, Y., Ebita, A., Moriya, M., Onoda, H. et al. (2015) The JRA-55
499 reanalysis: General specifications and basic characteristics. *Journal of the*
500 *Meteorological Society of Japan. Ser. II*, 93, 5-48.
501 Konôpka, B., Pajtík, J., Šebeň, V., Surový, P. & Merganičová, K. (2020) Biomass Allocation
502 into Woody Parts and Foliage in Young Common Aspen (Populus tremula L.)—Trees
503 and a Stand-Level Study in the Western Carpathians. *Forests*, 11, 464.
504 Lambers, H. (1998) Chapin~ III, FS, and Pons, TL: Plant Physiological Ecology. Spinger-
505 Verlag, New York, pp. 10-25.
506 Levin, S. A. (1992) The problem of pattern and scale in ecology. *Ecology*, 73: 1943-1967.
507 Litton, C.M., Raich, J.W. & Ryan, M.G. (2007) Carbon allocation in forest ecosystems. *Global*
508 *Change Biology*, 13, 2089-2109.
509 Liu, L., Gudmundsson, L., Hauser, M., Qin, D., Li, S. & Seneviratne, S.I. (2020) Soil moisture
510 dominates dryness stress on ecosystem production globally. *Nature Communications*,
511 11, 1-9.
512 McCarthy, M. & Enquist, B. (2007) Consistency between an allometric approach and optimal
513 partitioning theory in global patterns of plant biomass allocation. *Functional Ecology*,
514 21, 713-720.
515 Menzel, A., Sparks, T.H., Estrella, N., Koch, E., Aasa, A., Ahas, R. et al. (2006) European

516 phenological response to climate change matches the warming pattern. *Global Change*
517 *Biology*, 12, 1969-1976.
518 Metcalfe, D.B., Meir, P., Aragão, L.E., Lobo-do-Vale, R., Galbraith, D., Fisher, R. et al. (2010)
519 Shifts in plant respiration and carbon use efficiency at a large-scale drought experiment
520 in the eastern Amazon. *New Phytologist*, 187, 608-621.
521 Myneni, R., Knyazikhin, Y. & Park, T. (2015) MOD15A2H MODIS/terra leaf area index/FPAR
522 8-Day L4 global 500m SIN grid V006. *NASA EOSDIS Land Processes DAAC*,
523 https://lpdaac.usgs.gov/products/mod15a2hv006/.
524 Pantin, F., Simonneau, T. & Muller, B. (2012) Coming of leaf age: control of growth by
525 hydraulics and metabolics during leaf ontogeny. *New Phytologist*, 196, 349-366.
526 Piao, S., Wang, X., Park, T., Chen, C., Lian, X., He, Y. et al. (2020) Characteristics, drivers and
527 feedbacks of global greening. *Nature Reviews Earth & Environment*, 1, 14-27.
528 Poorter, H., Niklas, K.J., Reich, P.B., Oleksyn, J., Poot, P. & Mommer, L. (2012) Biomass
529 allocation to leaves, stems and roots: meta-analyses of interspecific variation and
530 environmental control. *New Phytologist*, 193, 30-50.
531 Preece, C., Farré-Armengol, G., Llusià, J. & Peñuelas, J. (2018) Thirsty tree roots exude more
532 carbon. *Tree Physiology*, 38, 690-695.
533 Reich, P.B., Luo, Y., Bradford, J.B., Poorter, H., Perry, C.H. & Oleksyn, J. (2014) Temperature
534 drives global patterns in forest biomass distribution in leaves, stems, and roots.
535 *Proceedings of the National Academy of Sciences*, 111, 13721-13726.
536 Reich, P.B., Sendall, K.M., Stefanski, A., Rich, R.L., Hobbie, S.E. & Montgomery, R.A. (2018)
537 Effects of climate warming on photosynthesis in boreal tree species depend on soil

538 moisture. *Nature*, 562, 263-267.
539 Sardans, J., PeNUuelas, J., Estiarte, M. & Prieto, P. (2008) Warming and drought alter C and N
540 concentration, allocation and accumulation in a Mediterranean shrubland. *Global*
541 *Change Biology*, 14, 2304-2316.
542 Tilman, D. (2020) *Plant Strategies and the Dynamics and Structure of Plant*
543 *Communities.(MPB-26), Volume 26*. Princeton University Press.
544 Tjoelker, M. G., M. G. Tjoelker, P. B. Reich and J. Oleksyn. (1999) Changes in leaf nitrogen
545 and carbohydrates underlie temperature and CO_2 acclimation of dark respiration in five
546 boreal tree species. *Plant, Cell & Environment*, 22: 767-778.
547 Verger, A., Baret, F. & Weiss, M. (2011) A multisensor fusion approach to improve LAI time
548 series. *Remote Sensing of Environment*, 115, 2460-2470.
549 Vicca, S., Luyssaert, S., Peñuelas, J., Campioli, M., Chapin III, F., Ciais, P. et al. (2012) Fertile
550 forests produce biomass more efficiently. *Ecology Letters*, 15, 520-526.
551 Wehr, R., Munger, J.W., McManus, J.B., Nelson, D.D., Zahniser, M.S., Davidson, E.A. et al.
552 (2016) Seasonality of temperate forest photosynthesis and daytime respiration. *Nature*,
553 534, 680-683.
554 Yan, K., Park, T., Yan, G., Liu, Z., Yang, B., Chen, C. et al. (2016) Evaluation of MODIS
555 LAI/FPAR product collection 6. Part 2: Validation and intercomparison. *Remote Sensing*,
556 8, 460.
557 Yuan, W., Zheng, Y., Piao, S., Ciais, P., Lombardozzi, D., Wang, Y. et al. (2019) Increased
558 atmospheric vapor pressure deficit reduces global vegetation growth. *Science Advances*,
559 5, eaax1396.

Zhang, Y., Joiner, J., Alemohammad, S.H., Zhou, S. & Gentine, P. (2018) A global spatially contiguous solar-induced fluorescence (CSIF) dataset using neural networks. *Biogeosciences*, 15, 5779-5800.

Zhu, Z., Piao, S., Myneni, R.B., Huang, M., Zeng, Z., Canadell, J.G. et al. (2016) Greening of the Earth and its drivers. *Nature Climate Change*, 6, 791-795.

Figure legends

FIGURE 1 Trends in ΔLAI throughout leaf green-up period (GUP) and for each month of the GUP for 2000-2017. a, Trends in ΔLAI throughout GUP (ΔLAI is defined as the difference between the annual maximum LAI and LAI in the month before the start of the growing season). They are parameters of a1 in Eq. 2, same as subplots of b-d. Trends in ΔLAI for (b) April (monthly ΔLAI is defined as the difference between LAI in the focused month and LAI in the preceding month), (c) May, (d) June and (e) July. Panels a-e share the same color bar shown below e. The black dots in a-e indicate significant trends at $P<0.05$. The histograms in a-e are frequency distributions of the trend in ΔLAI, the sequences of four bars represent the percentages of pixels with non-significantly negative trends, significantly negative trends, non-significantly positive trends, and significantly positive trends, respectively. f, The dominant month (TDM) contributing the most to the positive ΔLAI trend in a. g, Durations between SOS and TDM ($Duration_{SOS\text{-}TDM}$). Only pixels with positive trends in a are shown in f and g. The pie charts in f and g indicate the proportions of each group.

FIGURE 2 Factors dominating the ΔLAI trends for each month during leaf green-up period. The dominant factor is defined as the variable with the highest partial correlation coefficient after controlling for the other variables. Only climatic variables (soil-moisture content (SM), temperature (Tem) and solar radiation (Rad)) are considered in a-h, and the three climatic variables and solar-induced chlorophyll fluorescence (SIF) in the focused month are considered in i-p. Dominant factors positively correlated with ΔLAI are shown in a-d (climate only) and i-h (climate and SIF), while those negatively correlated with ΔLAI are shown in e-h (climate only) and m-p (climate and SIF) from April to July. Four intervals of $|R|$ in [0 0.43], (0.43 0.50],

588 (0.50 0.62] and (0.62 1] for a-h and in [0 0.44], (0.44 0.51], (0.51 0.64] and (0.64 1] for i-p
589 correspond to *P* values in [0 0.01], (0.01 0.05], (0.05 0.1] and (0.1 1], respectively. The
590 preseason length corresponding to the climatic data used for analysis is shown in Fig. S3.
591
592 **FIGURE 3** Trends in modeled ΔLAI and their dominant driving factors for each month during
593 leaf green-up period. Trends in modeled ΔLAI in (a) April (monthly ΔLAI is defined as the
594 difference between LAI in a month and that in the preceding month), (b) May, (c) June and (d)
595 July for 2000-2007. Panels a-d share the same color bar shown below d. The black dots in a-d
596 indicate significant trends at $P<0.05$. The histograms in a-d are frequency distributions of the
597 trend in ΔLAI. e-t, Factors dominating the modeled ΔLAI trends for each month during leaf
598 green-up period. The dominant factor is defined as the variable with the highest partial
599 correlation coefficient after controlling for the other variables. Only climatic variables (soil-
600 moisture content (SM), temperature (Tem) and solar radiation (Rad)) are considered in e-l, and
601 the three climatic variables and gross primary productivity (GPP) for the focused month are
602 considered in m-t. Dominant factors positively correlated with ΔLAI are shown in e-h (climate
603 only) and m-p (climate and GPP), and dominant factors negatively correlated with ΔLAI are
604 shown in i-l (climate only) and q-t (climate and GPP). Four intervals of $|R|$ in [0 0.43], (0.43
605 0.50], (0.50 0.62] and (0.62 1] for a-h and in [0 0.44], (0.44 0.51], (0.51 0.64] and (0.64 1] for
606 i-p correspond to *P* values in [0 0.01], (0.01 0.05], (0.05 0.1] and (0.1 1], respectively. The
607 preseason length corresponding to the climatic data used for analysis is shown in Fig. S9.
608
609 **FIGURE 4** Schematic of the climatic regulation of foliar C accumulation. The allocation of C
610 to leaves (C_{leaf}) is determined by both the total amount of assimilated photosynthetic C (C_{total})

and the proportion of C allocated to leaves (P_{leaf}), i.e. $C_{leaf} = C_{total} \times P_{leaf}$. (I) The accelerating accumulation of foliar C in the early stage of green-up is attributed to increases in photosynthesis and P_{leaf}. (II) The negative trend in the accumulation of foliar C in the late stage is mainly due to a decrease in P_{leaf} driven by climate but is weakly linked with photosynthesis. Potential mechanisms by which climate regulates P_{leaf} are shown in the ovals, where red arrows indicate positive effects and blue arrows indicate negative effects. Models overestimate the link between photosynthesis and the allocation of C to leaves and skew the change in P_{leaf} under climate change, which leads to mismatches between the models and satellite observations for the ΔLAI trend in the late stage of green-up period.

621 **Fig. 1**

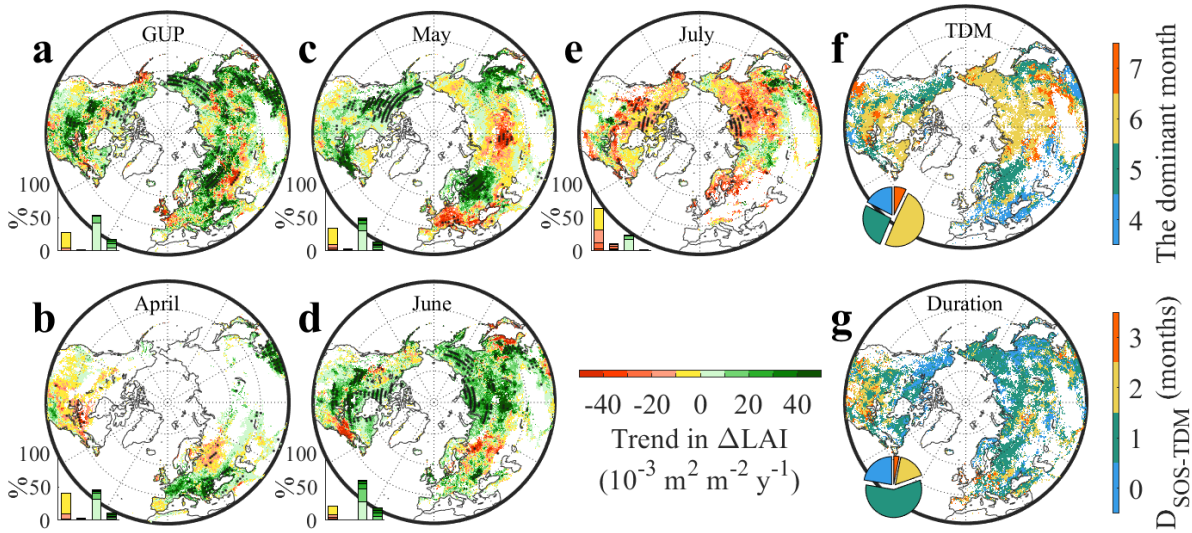
a
GUP
c
May
e
July
f
TDM
b
April
d
June
g
Duration
100
%50
0
-40 -20 0 20 40
Trend in ΔLAI
(10-3 m2 m-2 y-1)
7
6
5
4
The dominant month
3
2
1
0
DSOS-TDM (months)

622

623 **Fig. 2**

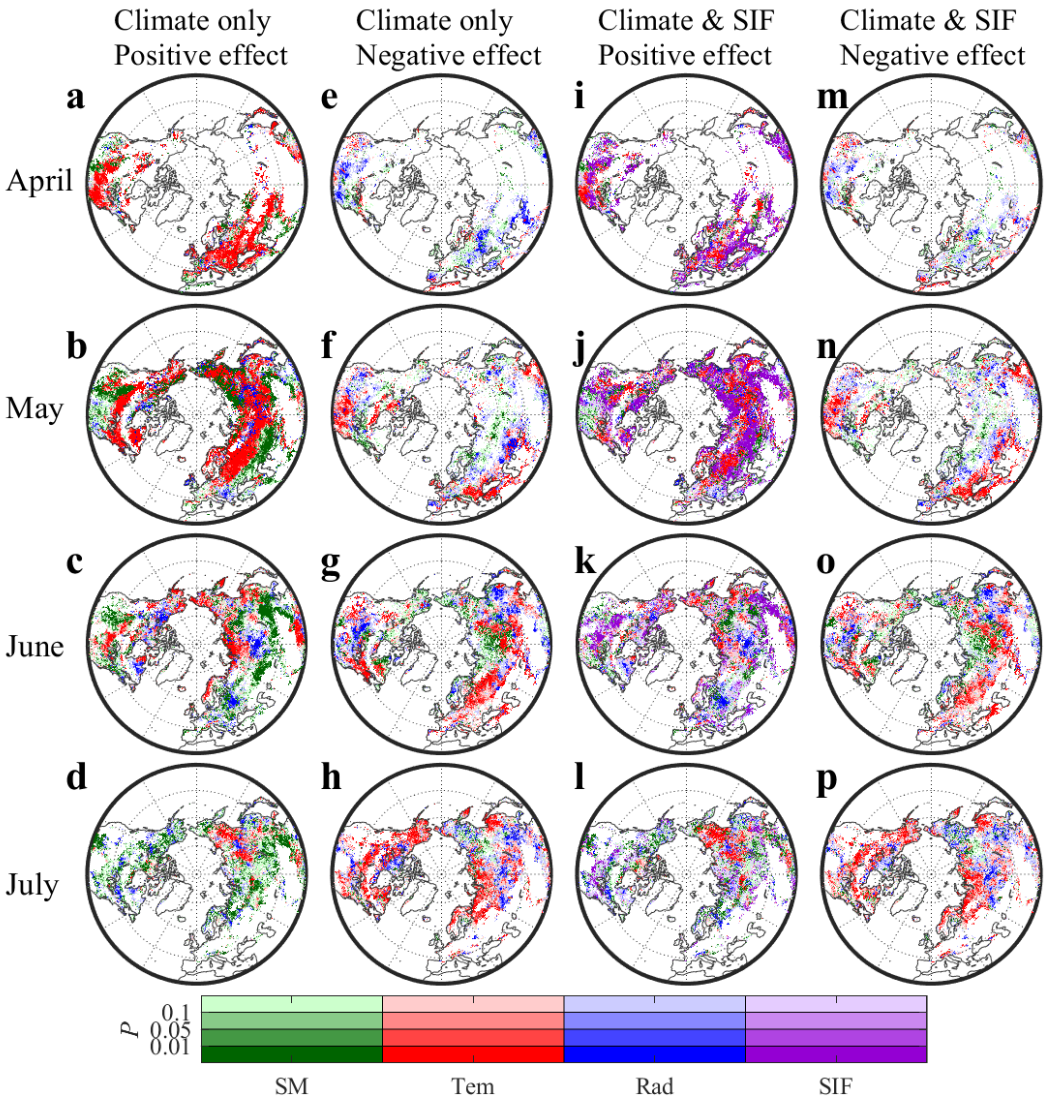
Climate only
Positive effect
Climate only
Negative effect
Climate & SIF
Positive effect
Climate & SIF
Negative effect
a
e
i
m
April
b
f
j
n
May
c
g
k
o
June
d
h
l
p
July
P
0.1
0.05
0.01
SM
Tem
Rad
SIF

624

625 **Fig. 3**

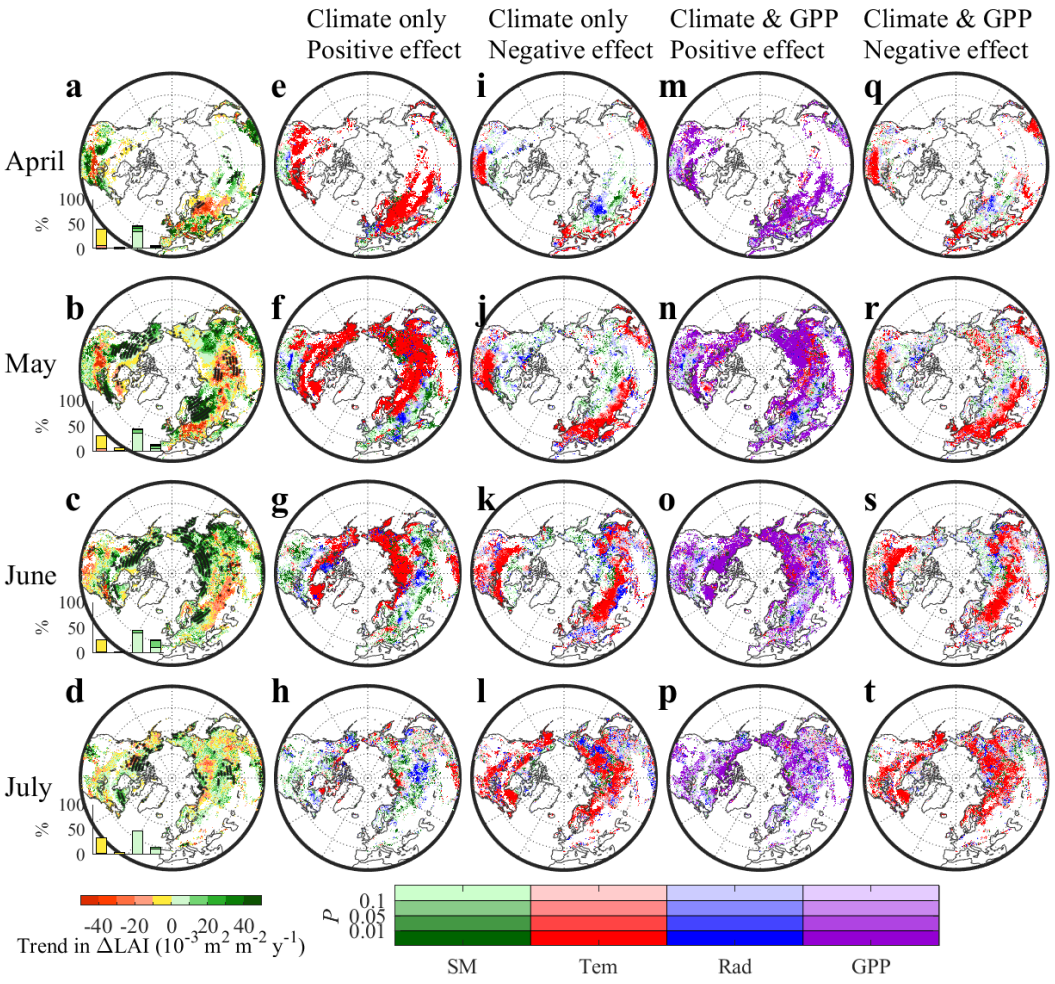

626

627

628 **Fig. 4**

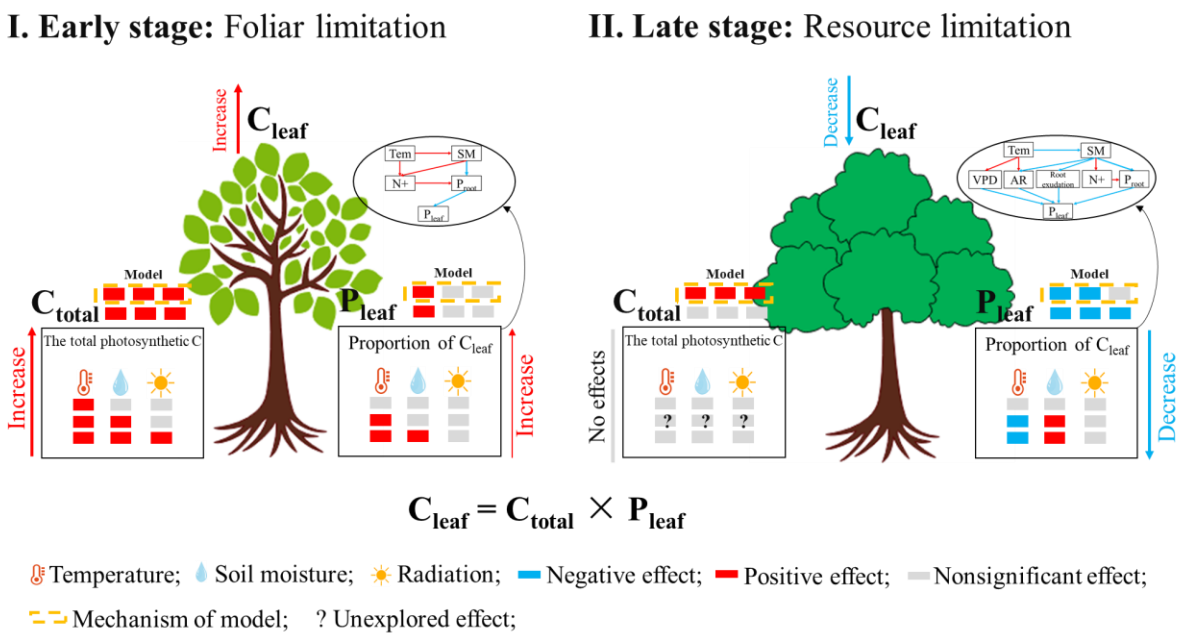

629

630